ChemComm

Chemical Communications

Accepted Manuscript

This article can be cited before page numbers have been issued, to do this please use: M. Singh, S. Sproules and J. Love, *Chem. Commun.*, 2026, DOI: 10.1039/D5CC06420A.

ROYAL SOCIETY OF CHEMISTRY

rsc.li/chemcomm

Stabilisation and characterisation of a trinuclear uranyl complex by ligand-radical formation.

Mukesh K Singh,*[a] Stephen Sproules,[b] and Jason B Love*[a]

Received 00th January 20xx,
Accepted 00th January 20xx

DOI: 10.1039/x0xx00000x

Redox-active ligands can play an important role in the chemistry of actinide complexes by facilitating alternative reaction pathways or modifying electronic properties. In this regard, we report here the synthesis of the first trinuclear uranyl complex of a bridging radical ligand, [K(18-c-6)][$(UO_2Cl_2)_3$(TPymT)] 4.25THF (1). Structural and electronic characterisation reveals delocalisation of the radical across the bridging ligand and that the stability of the complex is entirely dependent on radical formation, with oxidation resulting in uranyl decomplexation. This study highlights the interplay between radical chemistry and actinide complexes and opens up new avenues for further research in this area.

The integration of metal and organic radicals into molecular architectures is pivotal in developing materials with exceptional electronic and magnetic properties.[1] Previous studies on transition and lanthanide-metal radical complexes have revealed their potential in a range of applications, such as catalysis, magnetism, spintronics, molecular electronics, and medicine.[1-2] The radical centers within these complexes facilitate unique reaction pathways that significantly enhance catalytic efficiency and selectivity,[2b] while also contributing to novel magnetic properties crucial for high-density storage media.[3] The direct radical-metal interaction is known to enhance intramolecular magnetic exchange coupling, mitigating quantum tunnelling of magnetisation and elevating the energy barrier for spin reversal.[3]

In contrast, actinide-based radical complexes remain underexplored, with only a few reports on monometallic and dimetallic actinide-radical systems.[4] Notably, the scarcity of triactinide-bridged radical complexes and the absence of triuranyl-bridged radical complexes in the literature highlights a gap in knowledge.[5] In pursuit of suitable bridging ligands for the creation of trimetallic radical-bridged complexes, we identified 2,4,6-tris(2-pyrimidyl)-1,3,5-triazine (TPymT) as a promising candidate. Although TPymT has a rich 3d/4d/5d coordination chemistry and the capacity to coordinate three metal centers, its potential in actinide chemistry is largely unexamined, particularly with respect to its ability to form radical anions ($TPymT^{\bullet}$).[6]

Among actinide complexes, the uranyl dication, $[UO_2]^{2+}$, represents the least radioactive and most readily available actinyl ion, positioning it as the most extensively studied species within this category.[7] As the most thermodynamically stable form of uranium found in nature, it emerges as a significant soluble contaminant associated with nuclear waste, raising considerable environmental concerns. The structural characteristics of the uranyl ion are defined by two linear, exceptionally strong U–O bonds due to the overlap of U 5f and 6d orbitals with O 2p orbitals, resulting in one σ bond and two π bonds, culminating in a formal bond order of three. Furthermore, the importance of uranyl $[UO_2]^{2+}$ and its facile reduction, which facilitates catalytic activities, has become widely acknowledged.[8]

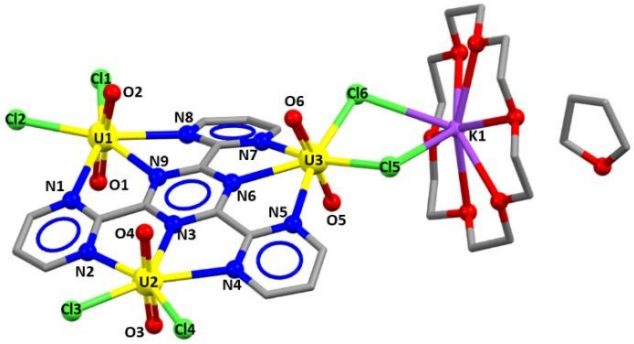

Fig. 1: The X-ray crystal structure of [K(18-c-6)][$(UO_2Cl_2)_3$(TPymT)] 4.25THF (**1**). For clarity, all hydrogen atoms and 3.25 THF solvent molecules are omitted. Selected bond distances and angles are summarised in Table S1.

With this in mind, we have synthesised and characterised the new TPymT-radical anion-bridged tri-uranyl chloride complex, [K(18-c-6)][$(UO_2Cl_2)_3$(TPymT)] 4.25THF (**1**). This compound represents the first example of a TPymT-anion radical-bridged trimetallic actinide complex. This study not only contributes to the understanding of radical-bridged actinide organometallic chemistry but also opens the possibility of new avenues for exploring the unique properties of actinide complexes, particularly in stabilising low oxidation states of uranium and enhancing magnetic exchange interactions.

RESULTS AND DISCUSSION

Stirring a mixture of TPymT (1 eq.), potassium graphite (1 eq.), 18-c-6 (1 eq.) and $[UO_2Cl_2(THF)_3]$ (3 eq.) in THF in the absence of light at room temperature results in the formation of **1**, which is isolated as dark blue needles after concentration of the solution and cooling to –20 °C. When the reaction is undertaken

[a] *EaStCHEM School of Chemistry, University of Edinburgh, EH9 3FJ, Edinburgh, UK. msingh2@ed.ac.uk; Jason.love@ed.ac.uk*
[b] *School of Chemistry, University of Glasgow, G12 8QQ, Glasgow, UK. stephen.Sproules@glasgow.ac.uk*

Electronic Supplementary Information (ESI) available: ccdc number for complex **1** is Deposition Number 2416326. [Experimental and computational details and spectral data are available]. See DOI: 10.1039/x0xx00000x

in the absence of potassium graphite and 18-c-6, no interaction between the uranyl precursor and the TPymT ligand is seen. The X-ray crystal structure of **1** was solved to reveal an intimate ion pair comprising a triuranyl TPymT anion linked to a potassium cation solvated by 18-c-6 through the equatorial chlorides Cl5 and Cl6 (Fig. 1 and Fig. S1). The U-O_{yl} distances range between 1.746(3) – 1.761(3) Å, indicating slightly stronger U-O_{yl} bonding in **1** compared with $[UO_2Cl_2(THF)_3]$[9] (U-O_{yl} = 1.765(6) – 1.766(7) Å) and the related uranyl(VI) complex of terpyridine $[UO_2Cl_2(terpyridine)]$[10] (U-O_{yl} = 1.773 – 1.790 Å) (Table S1). It is clear from these metrics that the uranium centres in **1** are in the +6 oxidation state as uranyl(V) U-O_{yl} distances are usually >1.85 Å.[7a] The O_{yl}-U-O_{yl} angles for **1** are linear, ranging from 174.28(17)° to 176.15(16)°. Additionally, each U atom is coordinated to two chloride ions, with U-Cl distances ranging from 2.6383(12) to 2.6614(13) Å, which are shorter than the U-Cl distances seen in $[UO_2Cl_2(THF)_3]$ (2.687(3) – 2.698(2) Å) and $[UO_2Cl_2(terpyridine)]$ (2.674 Å), suggesting slightly stronger U-Cl bonds in **1**. The three uranyl dichloride groups in **1** coordinate to the three terpyridine pockets of the TPymT-anion ligand, with U···U separations between 6.7046(4) and 6.8266(5) Å. A potassium ion from the $[K(18\text{-c-}6)]^+$ counter cation coordinates to both Cl5 and Cl6 ions bound to U3. Adjacent $[(UO_2Cl_2)_3(TPymT)]$ molecules are found to interact through U=O···π(pyrazine) and U-Cl···H(TPymT) intermolecular interactions (Fig. S1-S2).

To further understand the U-O_{yl} bonding, Quantum Theory of Atoms in Molecules (QTAIM)[11] and Wiberg bond index analysis[12] were carried out for **1** and compared against $[UO_2Cl_2(THF)_3]$ and $[UO_2Cl_2(terpyridine)]$ (Table S2-S3). From the QTAIM data, the greater total electron density (ρ), along with negative Laplacian of electron density ($\nabla^2\rho$) and energy density (H(r)) at the U-O_{yl} bond critical point (BCP), suggests stronger polar covalent U-O_{yl} bonding in **1** compared with both

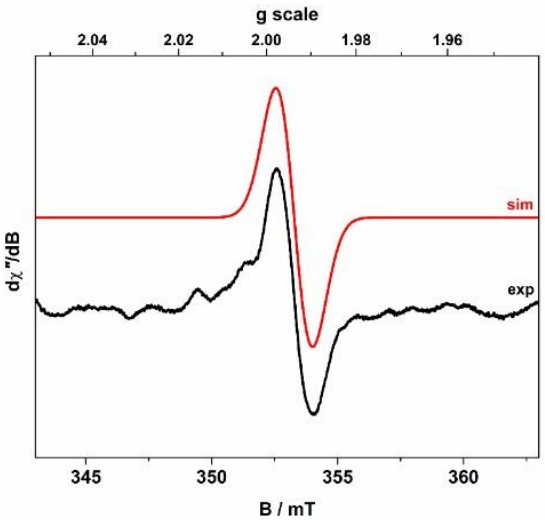

Fig. 2: X-band EPR spectrum of $[K(18\text{-crown-}6)][(UO_2Cl_2)_3(TPymT)]$ 4.25THF (**1**) recorded in THF solution at ambient temperature (experimental conditions: frequency, 9.8579 GHz; power, 6.3 mW; modulation, 0.4 mT). Experimental data are shown by the black line and simulation by the red trace.

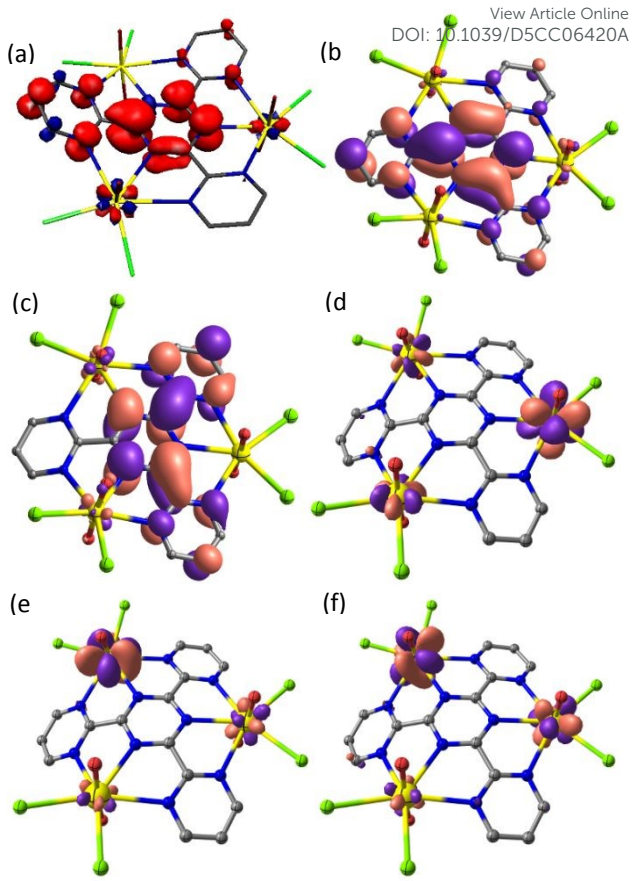

Fig. 3: DFT computed spin density plot showing radical-spin delocalised mainly on the triazine part of the TPymT ligand (a); and radical-based SOMO which shows predominantly ligand-centred π-character with minor metal d/f contribution (b), and [(LUMO) – (LUMO+3)] (c-f), respectively, for **1**.

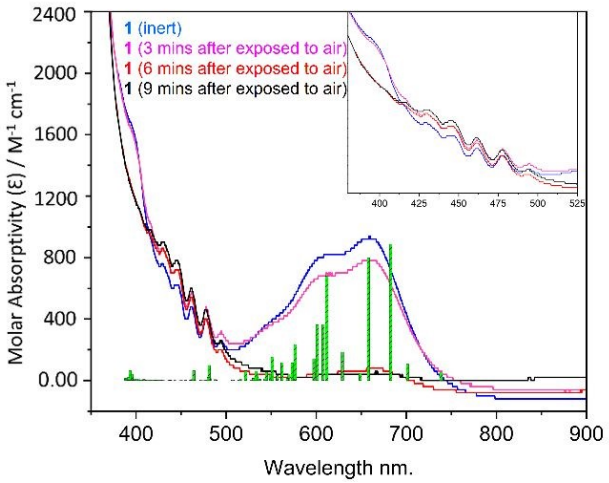

Fig. 4: UV-Vis-NIR absorption spectrum of **1** (THF, 350 – 900 nm) at different time intervals after the solution is exposed to air. The result of the time-dependent density functional theory (TDDFT) calculation of **1** is overlaid (green bars), suggesting TPymT-radical-based SOMO → U(5f) electronic transitions for most of these transitions, which disappear after exposure to air. The orbitals involved in the TPymT-radical-based SOMO → U(5*f*) electronic transitions are shown in Fig. S6 of ESI, which have more than 10% contributions.

View Article Online
DOI: 10.1039/D5CC06420A

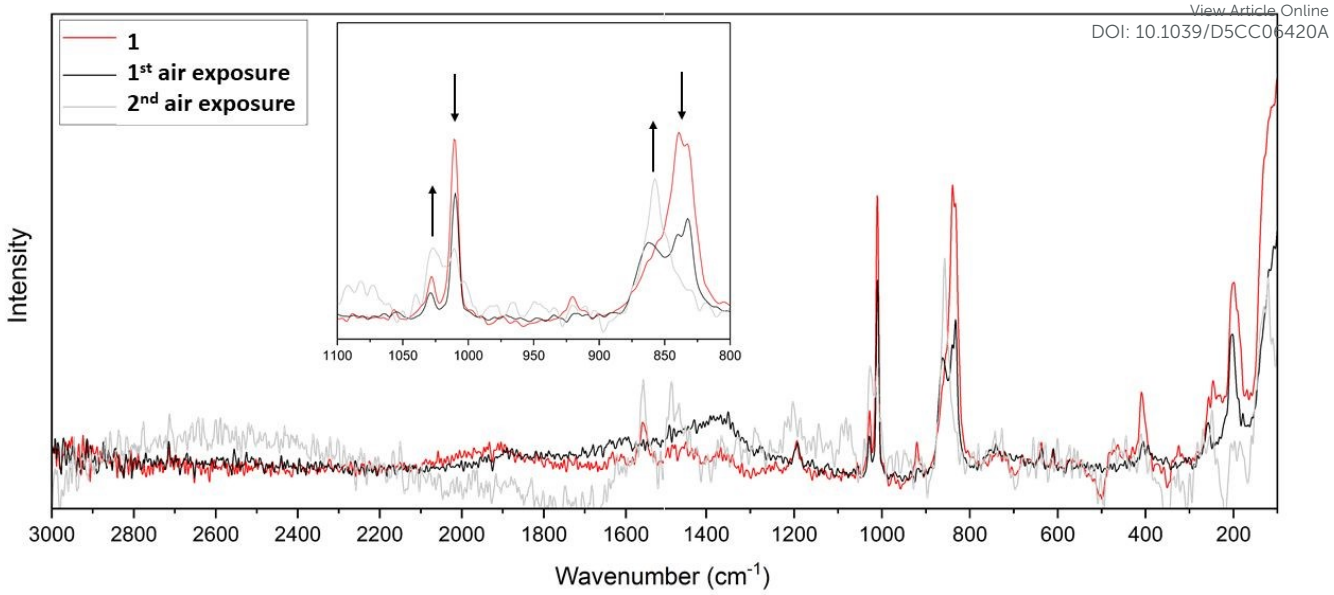

Fig. 5: Overlapped Raman spectra for Red: 1, Black:5 minutes and light-grey: 15 minutes, respectively, after exposing the solid sample to air.

$[UO_2Cl_2(THF)_3]$ and $[UO_2Cl_2(terpyridine)]$ (Table S2 and Fig. S3).[13] This is further supported by DFT-calculated Wiberg bond indices for the U-O_{yl} bonds of **1** of 2.1343-2.1914, which are found to be slightly greater than those of $[UO_2Cl_2(THF)_3]$ (2.1193-2.1439) and $[UO_2Cl_2(terpyridine)]$ (2.1554-2.1324) (Table S3). To explore the radical nature of **1**, its X-band EPR spectrum was recorded in THF and is found to display a resonance at g_{iso} = 1.9937, a value similar to other uranyl complexes bound to an organic radical ligand (Fig. 2).[14] In this case, the presence of the three U(VI) centres causes broadening of the resonance, obscuring any hyperfine interactions from protons or nitrogen. Additionally, the *g*-value is slightly decreased due to spin-orbit coupling effects.[14] Spin density analysis, computed using density functional theory (DFT) on **1**, indicates that the single electron is predominantly delocalised in π* orbitals of the 1,3,5-triazine moiety of the bridging ligand (Fig. 3) and specifically on the central triazene and a single pyrimidine arm with the shortest average U-N(pyrimidine) bonds.

The UV-Vis-NIR absorption spectrum for **1** in THF is characterised by two broad peaks in the range of 500 – 750 nm and several small, sharp stair-type peaks between 400 – 500 nm (Fig. 4). The calculated TDDFT spectra[15] of **1** indicate that most electronic transitions occurring in the range of 500 - 750 nm are associated with transitions from the singly occupied π*-triazine radical molecular orbital (SOMO) to LUMO unoccupied π*-triazine radical molecular orbital and empty uranium 5f-based molecular orbitals (Fig. S4-S6). Notably, after exposure of the solution of **1** to air for 10 seconds, measurements taken at three-minute intervals reveal the disappearance of these transitions (Fig. 4). Crystals grown from solutions of **1** exposed to air were identified as the uranyl starting material $[UO_2Cl_2(THF)_3]$. These observations show that the radical nature of the TPymT ligand is critical for uranyl coordination. To further investigate the spectroscopic characteristics of **1**, solid-state FTIR and Raman analyses were undertaken. The FTIR spectrum of **1** shows the U-O_{yl} asymmetric stretch (ν_3) at 912 cm^{-1} (Fig. S7), lower in energy relative to $[UO_2Cl_2(THF)_3]$ (939 cm^{-1}). A strong absorption at 1100 cm^{-1} is assigned to $[K\{18\text{-c-}6\}]^+$, similar to that reported previously.[16] The Raman spectrum of **1** exhibits a broad symmetric U-O_{yl} stretch (ν_1) at 830-840 cm^{-1} (Fig. 5 and S8). Additionally, a strong peak around 1010 cm^{-1} is seen that corresponds to metal-coordinated TPymT radical.[6i,17] Following exposure to air, measurements taken after 5 minutes and 15 minutes reveal a decrease in the intensity of the symmetric uranyl stretch (ν_1) and the vibrations of the TPymT radical with new absorptions at 858 cm^{-1} and 1025 cm^{-1} appearing and increasing in intensity. These latter peaks are attributed to the symmetric stretch (ν_1) of free uranyl and free ligand (TpymT), respectively, suggesting that **1** dissociates into starting materials upon exposure to air. In an attempt to reproduce both the Raman-active symmetric U-O_{yl} stretch (ν_1) and the IR-allowed U-O_{yl} asymmetric stretching (ν_3), DFT calculations on $[(UO_2Cl_2)_3(TpymT)]^{\bullet-}$ were carried out (Fig. S9 and ESI PowerPoint for the selected computed frequencies). Three Raman-active symmetric U-O_{yl} stretches (ν_1) are seen in the range of 853 to 871 cm^{-1}, while four IR-active asymmetric stretches (ν_3) are identified between 929 and 951 cm^{-1}. Additionally, four absorptions associated with the TpymT-radical ligand are found in the range 1037 to 1060 cm^{-1}. These calculated vibrations align well with the experimental data, with a slight shift of the calculated frequencies to the lower energy region.

In summary, the first trinuclear uranyl chloride complex of a TPymT radical anion was synthesised and characterised. Comprehensive structural, spectroscopic, and computational analyses underscored the radical nature of the complex and revealed its sensitivity to oxidation. This latter aspect highlighted the ability of the TPymT ligand to coordinate to uranyl solely as a ligand radical and not as a neutral ligand.

These results may contribute to the future design of novel materials with unusual catalytic and magnetic properties and provided insight into nuclear waste management.

Author Contributions

MKS undertook all of the experimental work and analytical characterisation, spectroscopic analysis, computation, and X-ray crystallography. SS performed the EPR analysis. MKS, SS, and JBL analysed the data and wrote the manuscript. JBL directed the research.

Conflicts of interest

There are no conflicts to declare.

Data availability

Experimental and computational details, along with additional data, are available in the supplementary information (ESI). The ESI PowerPoint file has the animations of the selected computed IR and Raman frequencies. See DOI: xxxxxxxx.

ACKNOWLEDGMENT

The authors thank the University of Edinburgh for funding. This work has made use of the resources provided by the Edinburgh Compute and Data Facility (ECDF) (http://www.ecdf.ed.ac.uk/). MKS would like to thank Gary S Nichol for his help solving the X-ray crystal structure.

References

1. (a) I. Ratera and J. Veciana, *Chem. Soc. Rev.*, 2012, **41**, 303-349; (b) G. Valente, P. Ferreira, M. A. Hernández-Rodríguez, C. D. S. Brites, J. S. Amaral, P. Zelenovskii, F. A. A. Paz, S. Guieu, J. Rocha and M. Souto, *Chem. Mater.*, 2024, **36**, 1333-1341; (c) L. Ji, J. Shi, J. Wei, T. Yu and W. Huang, *Adv. Mater.*, 2020, **32**, 1908015; (d) M. Mas-Torrent, N. Crivillers, V. Mugnaini, I. Ratera, C. Rovira and J. Veciana, *J. Mater. Chem.*, 2009, **19**, 1691-1695.

2. (a) X. Cui, Z. Zhang, Y. Yang, S. Li and C. Lee, *Exploration*, 2022, **2**, 20210264; (b) W.-C. C. Lee and X. P. Zhang, *Angew. Chem. Int. Ed.*, 2024, **63**, e202320243.

3. (a) S. Demir, I.-R Jeon, J. R. Long and T. D. Harris, *Coord. Chem. Rev.*, **289-290**, 149-176; (b) J. D. Rinehart, M. Fang, W. J. Evans and J. R. Long, *J. Am. Chem Soc.*, 2011, **133**, 14236-14239; (c) S. Demir, J. M. Nippe and J. R. Long, *J. Am. Chem Soc.*, 2012, **134**, 18546-18549; (d) I.-R. Jeon, J.G. Park, D.J. Xiao and T.D. Harris, *J. Am. Chem. Soc.*, 2013, **135**, 16845-16848; (e) M. K. Singh, *Dalton Trans.*, 2020, **49**, 4539–4548; (f) M. K. Singh, N. Yadav and G. Rajaraman, *Chem. Commun. (Camb)*, 2015, **51**, 17732-17735.

4. (a) S. J. Kraft, P. E. Fanwick and S. C. Bart, *Inorg. Chem.*, 2010, **49**, 1103; (b) S. C. Bart, F. W. Heinemann, C. Anthon, C. Hauser and K. Meyer, *Inorg. Chem.*, 2009, **48**, 9419-9426; (c) J. T. Coutinho, M. A. Antunes, L. C. J. Pereira, J. Marcalo and M. Almeida, *Chem. Commun.*, 2014, **50**, 10262-10264; (d) I. Castro-Rodriguez, H. Nakai, L. N. Zakharov, A. L. Rheingold and K. Meyer, *Science*, 2004, **305**, 1757-1759; (e) O. P. Lam, C. Anthon, F. W. Heinemann, J. M. O'Connor and K. Meyer, *J. Am. Chem. Soc.*, 2008, **130**, 6567-6576; (f) T. Mehdoui, J.-C. Berthet, P. Thuéry, L. Salmon, E. Rivière and M. Ephritikhine, *Chem. Eur. J.*, 2005, **11**, 6994-7006; (g) G. Zi, L. Jia, E. L. Werkema, M. D. Walter, J. P. Gottfriedsen and R. A. Andersen, *Organometallics*, 2005, **24**, 4251-4264; (h) E. M. Matson, S. R. Opperwall, P. E. Fanwick and S. C. Bart, *Inorg. Chem.*, 2013, **52**, 7295-7304.

5. L. Barluzzi, S. P. Ogilvie, A. B. Dalton, P. Kaden, R. Gericke, A. Mansikkamäki, S. R. Giblin and R. A. Layfield, *J. Am. Chem. Soc.*, 2024, **146**, 4234-4241.

6. (a) D. A. Safin, A. Pialat, I. Korobkov and M. Murugesu, *Chem. Eur. J.*, 2015, **21**, 6144-6149; (b) E. I. Lerner and S. J. Lippard, *Inorg. Chem.*, 1977, **16**, 1537-1546; (c) D. A. Safin, R. J. Holmberg, K. M. N. Burgess, K. Robeyns, D. L. Bryce and M. Murugesu, *Eur. J. Inorg. Chem.*, 2015, **2015**, 441-446; (d) A. M. Garcia, D. M. Bassani, J.-M. Lehn, G. Baum and D. Fenske, *Chem. Eur. J.*, 1999, **5**, 1234-1238; (e) T. Shiga, H. Miyamoto, G. N. Newton and H. Oshio, *Dalton Trans.*, 2018, **47**, 13402-13407; (f) J. M. Frost, L. Kobera, A. Pialat, Y. Zhang, S. A. Southern, B. Gabidullin, D. L. Bryce and M. Murugesu, *Chem. Commun.*, 2016, **52**, 10680-10683; (g) D. A. Safin, N. A. Tumanov, A. A. Leitch, J. L. Brusso, Y. Filinchuk and M. Murugesu, *CrystEngComm*, 2015, **17**, 2190-2195; (h) D. A. Safin, A. Pialat, A. A. Leitch, N. A. Tumanov, I. Korobkov, Y. Filinchuk, J. L. Brusso and M. Murugesu, *Chem. Commun.*, 2015, **51**, 9547-9550; (i) D. A. Safin, K. M. N. Burgess, I. Korobkov, D. L. Bryce and M. Murugesu, *CrystEngComm*, 2014, **16**, 3466-3469; (j) D. A. Safin, Y. Xu, I. Korobkov, D. L. Bryce and M. Murugesu, *CrystEngComm*, 2013, **15**, 10419-10422; (k) C. Lete, D. Visinescu, S. Shova, C. Maxim and M.-G. Alexandru, *J. Solid State Chem.*, 2022, **313**, 123292; (l) C. Maxim, A. Matni, M. Geoffroy, M. Andruh, N. G. R. Hearns, R. Clérac and N. Avarvari, *New J. Chem.*, 2010, **34**, 2319-2327.

7. (a) B. E. Cowie, J. M. Purkis, J. Austin, J. B. Love and P. L. Arnold, *Chem. Rev.*, 2019, **119**, 10595-10637; (b) E. J. Coughlin, Y. Qiao, E. Lapsheva, M. Zeller, E. J. Schelter and S. C. Bart, *J. Am. Chem. Soc.*, 2019, **141**, 1016; (c) P. L. Arnold, J. M. Purkis, R. Rutkauskaite, D. Kovacs, J. B. Love and J. Austin, *ChemCatChem*, 2019, **11**, 3786; (d) M. Azam, S. I. Al-Resayes, A. Trzesowska-Kruszynska, R. Kruszynski, P. Kumar and S. L. Jain, *Polyhedron*, 2017, **124**, 177; (e) Q. Zhang, B. Jin, R. Peng, X. Wang, Z. Shi, Q. Liu, S. Lei and H. Liang, *Int. J. Photoenerg.*, 2017, 8041647; (f) J. G. West, T. A. Bedell and E. J. Sorensen, *Angew. Chem., Int. Ed.*, 2016, **55**, 8923.

8. van Rees, K. and Love, J.B. (2024). Actinide Complexes of Redox Non-innocent Ligands. In Redox-Active Ligands, M. Desage-El Murr (Ed.)., Wiley-Liss Inc., pp. 317-341.

9. M. P. Wilkerson, C. J. Burns, R. T. Paine and B. L. Scott, *Inorg. Chem.*, 1999, **38**, 4156-4158.

10. J. Lhoste, N. Henry, T. Loiseau, Y. Guyot and F. Abraham, *Polyhedron*, 2013, **50**, 321-327.

11. (a) T. Lu and F. Chen, *J. Comput. Chem.*, 2012, **33**, 580-592; (b) H. L. Schmider and A. D. Becke, *J. Mol. Struct. THEOCHEM.*, 2000, **527**, 51-61.

12. (a) L. K. Harper, A. L. Shoaf and C. A. Bayse, *ChemPhysChem*, 2015, **16**, 3886-3892; (b) I. Mayer, *J. Comput. Chem.*, 2007, **28**, 204-221; (c) K. B. Wiberg, *Tetrahedron*, 1968, **24**, 1083-1096.

13. I. S. Bushmarinov, A. L. Konstantin and A. Mikhail Yu, *Russ. Chem. Rev.*, 2009, **78**, 283.

14. (a) K. van Rees, E. K. Hield, A. Carpentier, L. Maron, S. Sproules and J. B. Love, *Inorg. Chem.*, 2022, **61**, 3249-3255; (b) K. van Rees, T. Rajeshkumar, L. Maron, S. Sproules and J. B. Love, *Inorg. Chem.*, 2022, **61**, 20424-20432.

15. T. J. N. Obey, M. K. Singh, A. B. Canaj, G. S. Nichol, E. K. Brechin and J. B. Love, *J. Am. Chem. Soc.*, 2024, **146**, 28658-28662.

16. (a) G. Socrates, *Infrared and Raman Characteristic Group Frequencies*, Wiley, 2004; (b) L. Vugrin, I. Halasz and H. Geneste, *New J. Chem.*, 2023, **47**, 7466-7469.

17. T. Marzo, D. Cirri, L. Ciofi, C. Gabbiani, A. Feis, N. D. Pasquale, M. Stefanini, T. Biver and L. Messori, *J. Inorg. Biochem.*, 2018, **183**, 101-106.

View Article Online
DOI: 10.1039/D5CC06420A

Data availability

Experimental and computational details, along with additional data, are available in the supplementary information (ESI). The ESI PowerPoint file has the animations of the selected computed IR and Raman frequencies. See DOI: xxxxxxxx.